

ERS Wind Scatterometer Commissioning and in-flight Calibration

Pascal Lecomte

Directorate of Application Programmes - Remote Sensing Exploitation Division
ESA / ESRIN, Via Galileo Galilei, 00044 Frascati, Italy
tel: ++39-6-941 80 670, fax: ++39-6-941 80 612
Email: pascal.lecomte@esrin.esa.it

Wolfgang Wagner

Space Application Institute,
EC Joint Research Centre, TP 440, 21020 (VA), Italy
tel: ++39-332-78-6153, fax: ++39-332-78-9074
Email: wolfgang.wagner@jrc.it

Abstract

On the 26th March 1996, the ERS-2 Scatterometer Commissioning Phase Working group declared that ERS-2 Scatterometer data were ready for distribution to end-users.

This was the last step after nearly one year of work, firstly to find a way to recover the scatterometer, and secondly to perform in-flight characterisation of the instrument.

Since then, the AMI instrument suffered some anomalies and is under constant scrutiny to continuously assess the data quality, developing when required new methods.

The scope of this paper is to present the objectives of the calibration and validation activities, to detail the methods used to fulfill these objectives, and to present a method for estimating the spatially variable noise level over land surfaces.

Introduction

On the 21st April 1995, some three years ago, the second European Remote sensing Satellite, ERS-2 was launched from Kourou in French Guyana (see Fig. 1).

A C-band Scatterometer is part of the payload of the two European Remote sensing Satellites ERS-1 and ERS-2. It has been primarily designed for the derivation of wind speed and direction information over the oceans, but it is also a powerful sensor for the study of land surface processes. Over land, large-scale terrain features, and to a lesser extent build-up areas and inland waters, are causing modest azimuthal effects in the ERS Scatterometer data. As these effects do not contain important information, it is proposed to consider them as a noise to be added to the instrument noise and to the speckle. After a discussion on the calibration and validation tools already in use at the European Space Agency, a user-friendly method is presented that allows to estimate the spatially variable standard error of ERS Scatterometer measurements due to these error sources over land (Wagner et al., 1998). The method described, allows a consistent assessment of the quality of ERS Scatterometer derived data products.

The ERS Scatterometer

The scatterometer on ERS satellites is combined with a Synthetic Aperture Radar (SAR) into a single Active Microwave Instrument (AMI). This instrument is operated in either SAR or scatterometer mode. Most of the time, the instrument is operated in wind/wave mode which consists of nominal Scatterometer operation interrupted every 30 seconds by a couple of seconds of short SAR operation in order to acquire small SAR imaggettes from which the wave spectra can be derived. This wind wave mode of operation is interrupted for SAR images acquisitions on end user request.

The ERS Scatterometer is a vertically polarised radar operating at 5.3 GHz (C-band). Since the launch of ERS-1 in 1991 it has been providing world-wide coverage with a spatial resolution of 50 km. It illuminates a

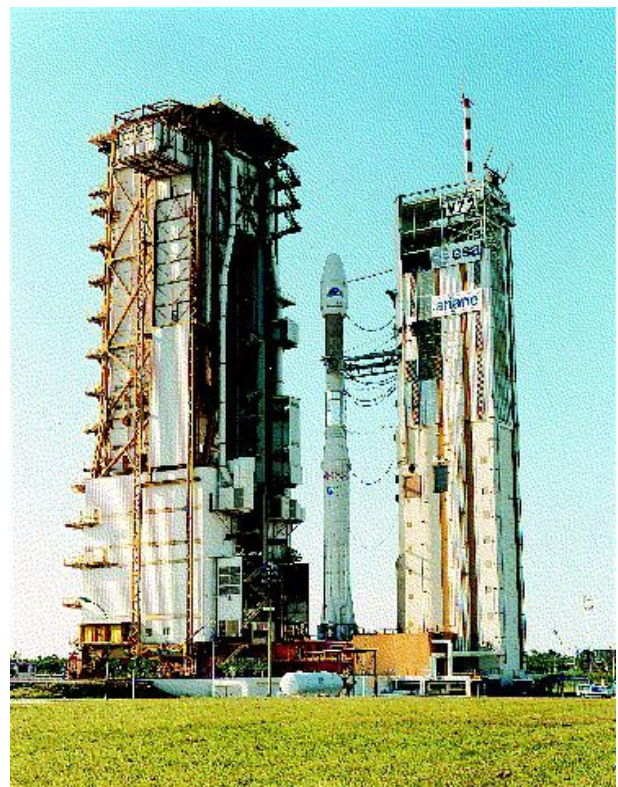


Figure 1: 21 April 1995: ERS-2 on the launch pad

500 km wide swath corresponding to an incidence angle range of 18 to 59°. Its three sideways looking antennas measure the backscattering coefficient from three different viewing directions. One antenna is looking normal to the satellite track, one is pointing 45° forward and one 45° backward with respect to the satellite track. Over ocean surfaces backscatter is modified by wind-driven ripples and the information acquired by looking from three different azimuth angles onto these ripples allows to derive wind speed and wind direction. ERS Scatterometer wind data are used operationally by meteorological offices (Stoffelen et al., 1993) for wind and wave forecasting and to support offshore operations and ship routing.

The ERS Scatterometer can also be used for monitoring land surface processes. Potential applications are soil moisture monitoring (Pulliainen et al., 1996; Wagner et al., 1996; Magagi and Kerr, 1997; Wagner, 1998), production of global vegetation maps (Frison and Mougin, 1996a and 1996b), and soil state monitoring in permafrost regions (Boehnke and Wismann, 1996). It is foreseen that one or the other application will become operational. To ensure high-quality geophysical data products the absolute radiometric calibration and the relative noise level of ERS Scatterometer measurements must be known.

First Scatterometer data

During the initial testing of the ERS-2 spacecraft, the first attempt to switch on the AMI resulted in a serious anomaly causing the instrument to shut down, both in SAR and Scatterometer modes. It was soon discovered that the instrument was prevented from working at nominal power. By reducing the output power to the minimum, engineers succeeded in acquiring the first SAR image on the same day, but it was still not possible to run the instrument in Wind mode.

Many tests were made to determine the cause and possible solutions to the problem. For more than six months the only data received from the scatterometer was limited to few calibration pulses and echoes at each test, with no more than six echoes in a row before the instrument shut down.

On the 29th September 1995 more echoes were received than during all the months since launch, when the instrument was operated for an entire orbit.

The anomaly was resolved by setting the redundancy switch at the input to the High Power Amplifier to an intermediate position, thereby using it as a voltage splitter. The output power was reduced by a factor of two, and, for the first time some wind measurements could be made.

After the resolution of a few minor problems involving the system stability in the new configuration, the instrument went into the everyday satellite operations plans on the 2nd of November 1995.

The Calibration subsystem

After a few months of nominal operation, a new anomaly affected the ERS-2 Scatterometer operations. The relay used to switch on and off the Calibration subsystem was not latching properly and more and more often the instrument was shutting down following a relay failure. On the 6th of August 1996 it was decided to operate the instrument with the redundant unit of the Calibration subsystem.

This change of configuration implied directly the necessity of re-calibrating the AMI in both SAR and Scatterometer mode. The detailed Analysis of the data before and after the switch showed two features, a bias which was initially measured to be around -0.16 dB and a power decrease of -0.24 dB per cycle since the instrument was operational. The bias had to be corrected by changing the level of the reference Calibration Pulse in one of the processing Look-Up-Tables. The drift was not expected as nothing like that was ever experienced with ERS-1.

It was first necessary to characterise which elements of the chain were producing this power decrease and in particular if the Calibration sub system was not directly involved. After a long analysis it was finally confirmed that the drift is entirely due to pulse generation and amplification part of the AMI, and that the Calibration sub/system is not contributing to it. This means that the same drift is observed in the echo and the Calibration pulse and that the final σ^0 is free of any drift as the echo is normalised by the Calibration pulse during the processing.

On the 18th June 1997, the Reference Calibration Pulse was corrected by 0.2 dB, 0.16 dB to correct for the different characteristics of the two Calibration sub-systems and 0.04 dB to correct the fact that ERS-2 was a bit low with respect to ERS-1.

Absolute and Relative Calibration

At the engineering level, the result of processed scatterometer data are radar backscattering coefficients, σ^0 , across the range of incidence angles of the instrument, for each of the three beams. These are then used to derive wind speed and direction using a backscatter to wind model (inversion).

The objectives of engineering calibration are to ensure that the σ^0 which is expected from a known target, is measured by the instrument (absolute calibration), and that the variation over the range of incidence angles of the instrument is unaffected by the local attenuation from the antennae (relative calibration).

When ERS-1 was launched, it was agreed that an absolute radiometric calibration of 0.7 dB was enough to satisfy the geophysical data quality requirements in terms of wind speed and direction (Instrument specification). Following the Calibration subsystem anomaly it

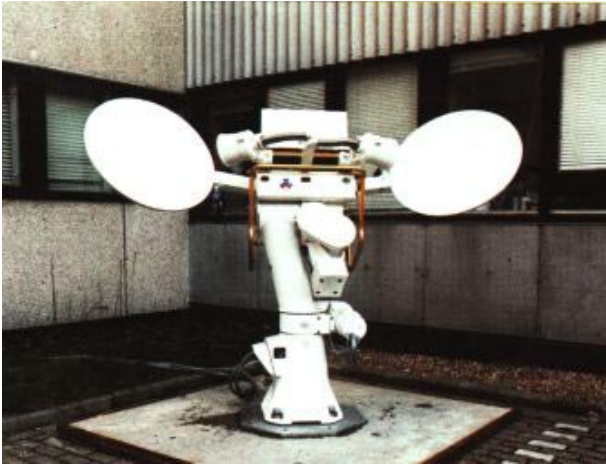


Figure 2: Scatterometer Transponder during testing at Estec

became clear that the meteorologist can detect in the wind fields a bias corresponding to less than 0.2 dB.

This requirement is translated into three elements:

- the radiometric stability
- the absolute calibration
- the relative calibration across the swath for a given antenna (antenna patterns) and between the different antennae

This is achieved by using a combination of internal (for the radiometric stability) and external references (Lecomte and Attema 1992). Two different types of external references are used, point targets (transponders) and distributed targets (areas of known, constant backscatter), addressing respectively the absolute and the relative calibration.

Three transponders, one of them shown on Fig. 2 during testing at Estec, are installed in the South of Spain (Fig. 3). This position facilitates measurements at two or more incidence angles every three days. They are



Figure 3: Scatterometer Transponder Location South of Spain

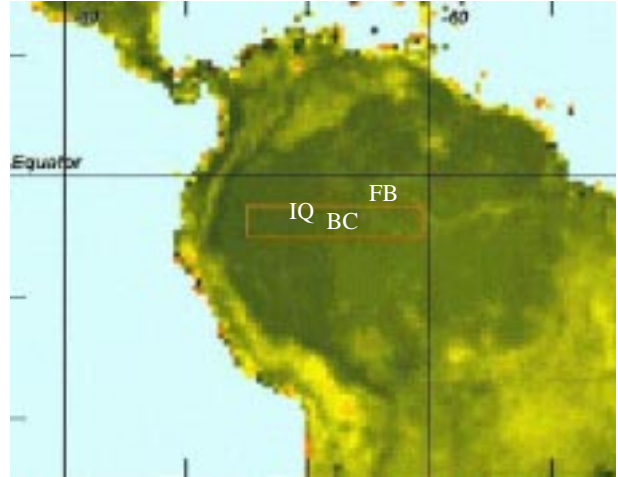


Figure 4: Amazonian Forest: Test area

arranged in a line, spaced over hundreds of kilometers, such that all three may be illuminated by each scatterometer beam during an ascending or a descending pass. Additionally, passes where two transponders are illuminated by one or more beams are used.

Each pass over a transponder allows the measurement error in backscatter at a particular incidence angle, to be computed from the power of the returned signal, and that measured at the transponder. The observation time of the transponders (in range and in azimuth) is used to verify proper antennae pointing.

After ERS-2 commissioning, two transponders will remain for monitoring purposes.

Although the transponders give accurate measurements of antenna attenuation at particular points within the antenna pattern, they are not adequate for fine tuning across all incidence angles, as there are simply not enough samples. This could be solved by deploying and operating a large number of transponders, so that many measurements can be made across the entire swath. Fortunately this enormous expense can be avoided by making use of large scale natural targets with a known response.

The tropical rain forest in South America has been used as a reference distributed target. The target is assumed to be isotropic and time invariant. Radar backscatter from the rain forest is shown on Fig. 4, as it was imaged by the ERS-2 Scatterometer. This image shows the σ^0 of the rain forest corrected for the effect of illuminating the scene over a range of incidence angles. This demonstrate clearly the uniform rain forest radar backscattering signature. Rivers, towns and montains have a lower or higher σ^0 and consequently show up as dark or bright patches in the image.

The primary goal of the ERS-2 Scatterometer calibration was to provide continuity to the users of the ERS-1 Scatterometer data. It was assumed that once the engineering calibration was complete, in terms of σ^0 , that the wind derivation, and in particular the C-Band model used to compute the wind from the σ^0 , was identical

Prior to the launch, the engineering parameters such as the antenna pattern or the on-board gain, were set using the results of the on-ground characterisation of the instrument. Following launch, and the subsequent recovery of the instrument, the transmit power was lower, due to the initial anomaly.

The commissioning phase activities were then limited to the following activities:

- Set the on-board receiver gain,
- Derive the antenna pattern correction for the three antennae from the rain forest and transponder measurements,
- Compute the antennae mispointing,
- Compute the calibration coefficients, and generate the associated Look-Up-Tables,
- Verify the stability of ERS-2 raw data (monitoring of the Long Term Stability of the instrument),
- Compare the ERS-1 and ERS-2 response over rain forest and transponders.

Receiver Gain Setting

ERS-1 on-board gains were optimised to ensure maximum use of the dynamic range of the analog to digital converter (ADC), whilst avoiding saturation. The initial ERS-2 on-board gains were set to the same level as for ERS-1.

The operational ERS-2 transmit power is approximately half the original setting, and also that of ERS-1. The configuration of the on-board receiver gain was not changed at the beginning of the commissioning phase. This allowed the stability of the instrument to be monitored for a number of months after operation began.

The ERS Scatterometer processing is independent of the receiver gain setting, and small variations in on-board transmit power. This is achieved by scaling the incoming echoes by the ratio of the expected calibration pulse level, against the calibration pulse measured on-board at the same moment. Thus changing the receiver gain, result in an increase or decrease in the echoes, and a similar effect in the measured calibration pulses.

Once the first corrections to the antenna patterns were made, and the stability of the instrument verified, the receiver gain was modified from 18 to 21 dB to take full advantage of the ADC dynamic range.

Antennae Mispointing

Two of the three scatterometer antennae on ERS are mechanically deployed. Small mispointing errors of the antennae may be corrected for in the ground processing. The orientation of the normal of each antenna plane can be determined using the transponders, by measuring the difference between the time the peak signal of each beam is observed, and when they are expected.

This analysis performed on ERS-2 Scatterometer data shows that the mispointing is negligible.

Antenna patterns

The in-flight antenna patterns are characterised using a combination of single point measurements from the transponders, and measuring the response over a known, stable distributed target.

For C-Band microwaves (5.3 GHz) tropical rain forests may be regarded as pure volume scatterers for which the incoming signal is equally scattered in all directions. Consequently, for the angle of incidence used by the ERS Scatterometers, the normalised backscattering coefficients σ^0 will depend only on the surface effectively seen by the instrument.

This surface S' is directly linked to the incidence angle by the relation

$$S' = S \cdot \cos \theta \quad 1$$

Definition of γ^0

One can define the following formula:

$$\gamma_{linear}^0 = \frac{\sigma_{linear}^0}{\cos \theta} \quad 2$$

Using this relation, the γ^0 backscattering coefficients over the rain forest are independent of incidence angle, allowing the measurements from each of the three beams to be compared.

Thus if the assumptions of this relation are correct, then the γ^0 over such a target should be flat across the entire swath, and equal in all beams.

An area was chosen, shown in Fig. 4, which exhibits:

- Flat topography. (The incidence angle θ is computed with respect to the ellipsoid GM6, and not with respect to the real topography).
- No large scale deforestation.
- No large rivers, lakes or towns.
- Stable climate. (Rain and humidity influence the backscattered signal).

This test area is located between 2.5°S and 5.0°S in latitude and 60.5°W and 75.0°W in longitude. This area is not touched by deforestation and has limited urbanisation, lies south of the Amazon, and north east of the main mountain ranges of South America. Furthermore, this area has a low rain variation over the year. In fact the comparison of the annual rain fall over the stations of Fonte Boa, Iquitos and Benjamin Constant (“FBV”, “IQ” and “BC” in Fig. 4) and other stations, shows that the annual variation is lower over the test area. Still, this variation is not negligible as the annual variation is higher than 200 mm at Benjamin Constant. At this station, the annual minimum is during the period June to Septembre.

Analysis of γ^0

The Fig. 5 shows a comparison of the γ^0 with respect to the incidence angle θ for the three beams of the ERS-

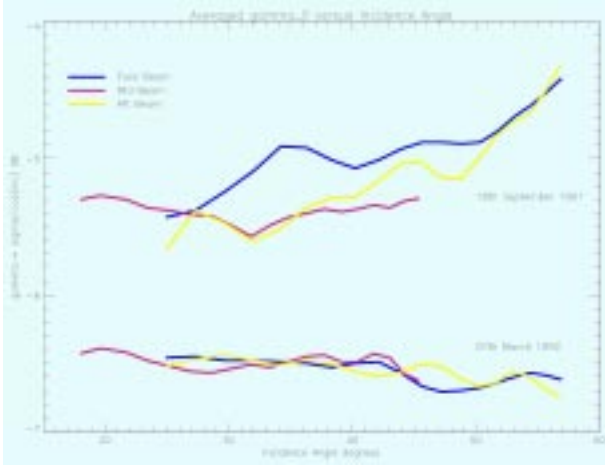


Figure 5: Average γ^0 over rain forest, before and after engineering Calibration

2 Scatterometer, before and after the instrument calibration.

The two side antennae (fore and aft) have nearly identical patterns. The deviation between the two curves are less than 0.3 dB. A more careful analysis of this data shows that the oscillation observed in these two curves can also be seen in the mid beam at an incidence angle 10° less. Thus it can be surmised that these anomalies correspond to the target and are probably due to small heterogeneity of the test area.

The second and the third nodes of the mid beam, which correspond respectively to an incidence angle of 19.6° and 21.7° , show a different effect. These two measurements give a value of γ^0 higher than that measured by the two other beams.

The deviation, +0.2 dB, is systematic and does not depend either on the period of the year, nor on the test area chosen. This may point to an anomaly in the characterisation of the mid antenna pattern.

The initial ERS-2 pattern corrections have produced satisfactory results, and a fine tuning is under way.

Instrument stability

The instrument calibration pulses are used to measure the stability of the transmit/receive chain on-board. As mentioned above, the scatterometer processing automatically corrects for any variation measured by the calibration pulses. Changes in the antenna patterns over time may also occur, in the long term due to temperature variation around the orbit, and throughout the year.

As γ^0 is independent of incidence angle, a histogram of γ^0 over the rain forest is characterised by a sharp peak. Monitoring the position of the peak over time is one method to check the stability of the calibration.

Histograms are produced, one for each antenna (“Fore”, “Mid”, and “Aft”) and one combining all measurements (“Fore/Mid/Aft”). The histogram bin size is 0.02 dB. The mean and the standard deviation are com-

puted directly from each distribution. The peak position is computed by fitting the histogram with a normal distribution added to a second order polynomial.

$$F(x) = A_0 \cdot \exp\left(-\frac{z^2}{2}\right) + A_3 + A_4 \cdot x + A_5 \cdot x^2 \quad 3$$

$$\text{with } z = \frac{x - A_1}{A_2} \quad 4$$

In this formulation, the normal distribution has a mean equal to A_1 and a standard deviation equal to A_2 . The parameters A_0 to A_5 are computed by using a non linear least square method called “gradient expansion” [Bevington, 1969].

The position of the peak is given by the maximum of the function F .

This method gives much more precise results than a simple filtering method.

The histograms (Fig. 6) computed for ERS-2 with one of the first set of calibrated data acquired at the beginning of April 1996 over the test area show the following points:

- Unique peak,
- The peak positions for all beams are nearly identical,
- The widths of the distributions are small (the standard deviations are lower than 0.35 dB).

The following table summarises the results for the end of March 1996.

γ^0	Mean	Peak position	Standard deviation
Fore	-6.48 dB	-6.44 dB	0.29 dB
Aft	-6.46 dB	-6.44 dB	0.28 dB
Mid	-6.61 dB	-6.56 dB	0.32 dB
All	-6.51 dB	-6.48 dB	0.30 dB

Table 1: ERS-2 γ^0 mean , peak position and standard deviation for end of March 1996

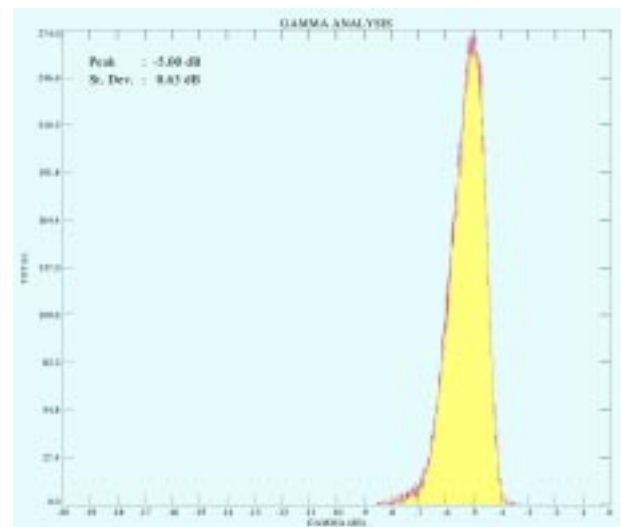


Figure 6: ERS-2 γ^0 distribution beginning of April 1996

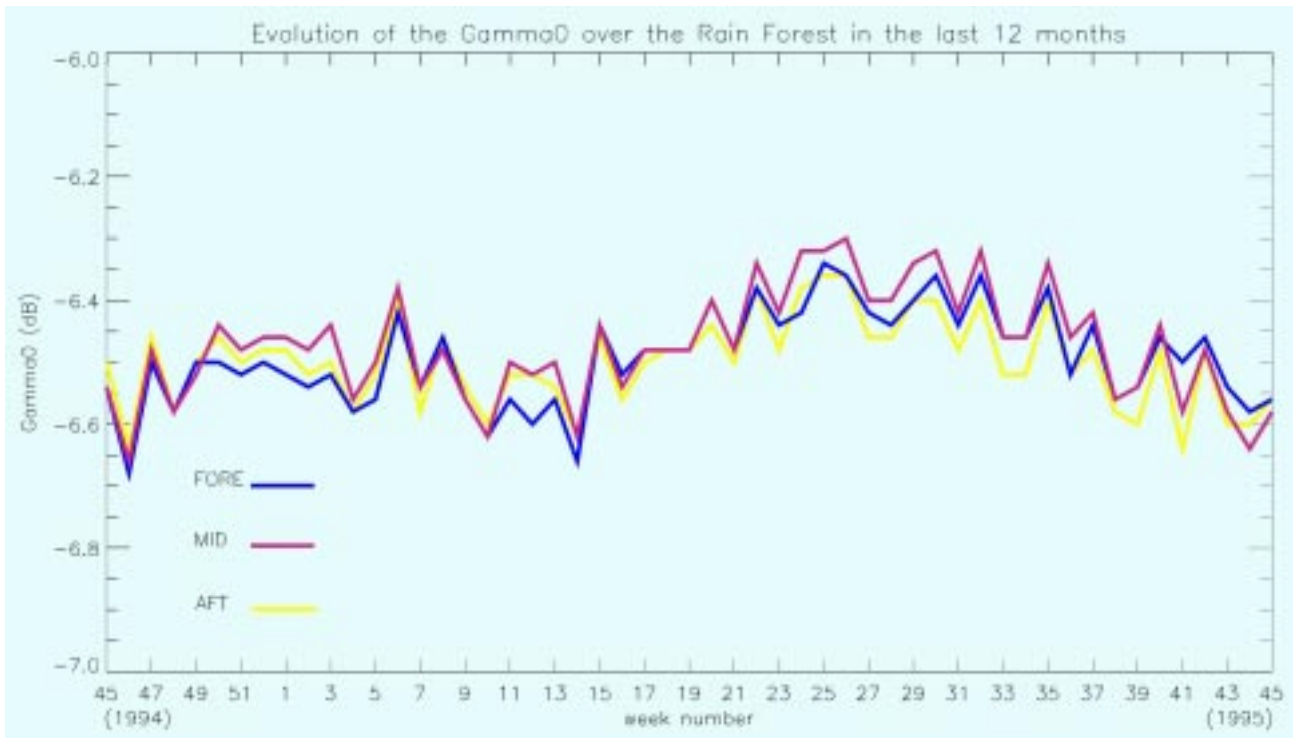


Figure 7: ERS-1 γ^0 distribution peak position time-series.

This demonstrates that the assumptions of the γ^0 have some foundation, and that γ^0 is useful as a comparison of the measurements made with the three antenna without having to take into account the incidence angles.

The following conclusions can be drawn:

- There is a slight deviation between the peak position and the mean of the distribution; i.e. that the distributions are not symmetrical.
- The standard deviation of the mid beam is higher than the two other antennae. This can be due to two reasons: first the noise on the mid beam is slightly higher. Secondly the higher γ^0 measured on the mid beam at low incidence angles (node two and three) is not corrected for when constructing the histograms and introduces noise in the γ^0 distribution.
- Taking into account the noise observed in the measurements, the peak position for the Fore and Aft antennae are equal; the mid beam has a slightly higher signal (+0.1 dB).

ERS-1 Annual stability

The Long term stability of the scatterometer is an important element of the Calibration activities. It has to be seen as the extension of the commissioning phase across the entire life time of the instrument.

For the ERS missions, the peak position of the γ^0 distribution is weekly monitored in parallel to the transponder activities.

The Fig. 7 shows the ERS-1 peak position time series for the three antennae over the period November 1992 to November 1993.

The analysis of these curves demonstrate the stability over the whole period, even if a small oscillation can be detected. It is also noteworthy that the three antennae have very similar responses. One can see a seasonal variation in all three antennae. This signal has an amplitude of 0.2 dB.

Comparisons of the γ^0 time-series with the rain fall measurements at Benjamin Constant show that the data do not correspond. The maximum γ^0 is separated by three months from the minimum rainfall.

Noise Level over Land Surfaces.

σ^0 Azimuthal Dependence

Backscatter from water surfaces and ice sheets depends on the azimuthal look direction. In the case of water the orientation of the water ripples with respect to the look direction of the sensor is important and in the case of ice the morphology of the surface and the top few meters of the snow and ice volume (Rott et al., 1993). On a field scale backscatter from vegetation might also exhibit an azimuthal dependence, but on larger scales these effects are not important. Nevertheless, azimuthal effects have been observed in the ERS Scatterometer data also over land surfaces (Wismann and Boehnke, 1994; Wagner, 1996). To investigate these effects in more detail the data acquired with the forward and backward looking antennas are analysed. These two antennas look at the surface with the same incidence angle, but from two different azimuth angles. Let us denote the backscattering coefficients acquired with the fore- and

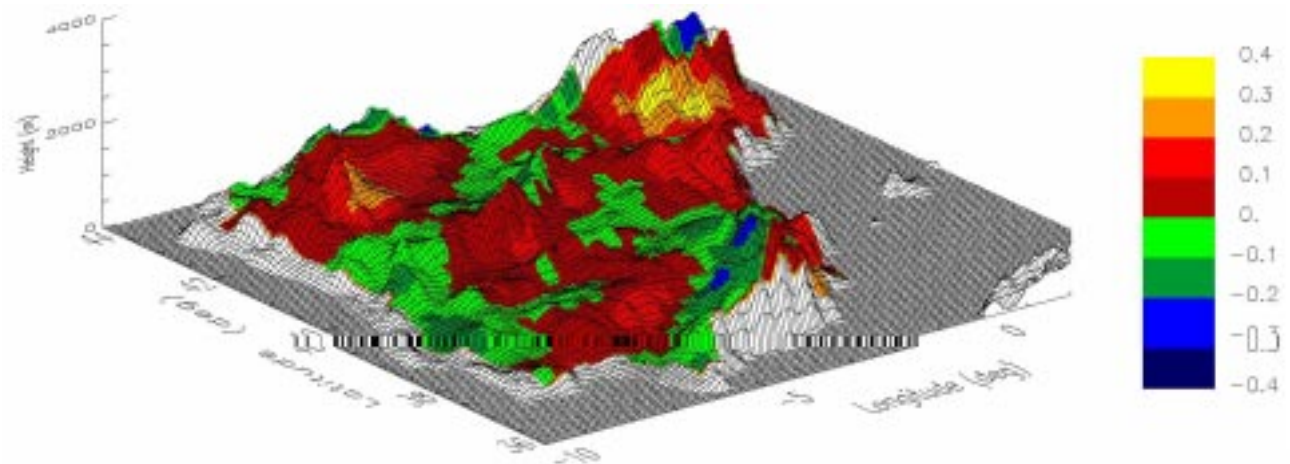


Figure 8: Overlay of δ (averaged value over ERS-1 mission) in dB for ascending passes over the DEM of the Iberian Peninsula

the aft-beam antennas with σ_{fore}^0 and σ_{aft}^0 respectively and let us take their difference:

$$\delta = \sigma_{fore}^0 - \sigma_{aft}^0 \quad 5$$

Since σ_{fore}^0 and σ_{aft}^0 are measured at the same incidence angle the difference δ depends on the noise level of individual σ^0 measurements and on the azimuthal dependence of σ^0 , but not on the backscattering characteristics of the target. If a large number of measurement pairs σ_{fore}^0 and σ_{aft}^0 are available then the noise can be averaged out and the resulting mean value of δ shows the magnitude of azimuthal effects. In Fig. 8 the average value of δ for ascending passes can be seen for the Iberian Peninsula. In the view of this figure, the look direction of the fore-beam antenna is approximately perpendicular to the plane of the page (south-west to north-east) and the look direction of the aft-beam antenna is approximately in the plane of the page from the left to the right (north-west to south-east). It can be observed that δ is positive over southward facing slopes where the local incidence angle of the forward looking antenna is smaller than the incidence angle of the backward looking antenna. The difference is positive because σ^0 is in general decreasing with the incidence angle and thus σ_{fore}^0 is larger than σ_{aft}^0 . Over northward facing slopes the reverse is true. Such it is clear that azimuthal effects as observed with the ERS Scatterometer are in reality incidence angle effects. Over the Iberian Peninsula the highest values of δ are around 0.4 dB. Over the Canadian Prairies δ is observed to be as large as 0.6 dB (Wagner, 1996).

Estimating the Noise Level

The three antennas of the ERS Scatterometer measure σ^0 from six different azimuth angles, three for the ascending and three for the descending node respectively. Over land the variation of σ^0 with the azimuth angle does not convey important information and thus

one may treat these rather modest variations as noise and the azimuth angle as “unknown”. Let us assume that in the logarithmic range σ_{fore}^0 and σ_{aft}^0 are normally distributed variables with equal means and with a standard deviation $S(\sigma^0)$. The means of σ_{fore}^0 and σ_{aft}^0 are determined by target characteristics and the standard deviation is due to all possible noise sources. The most important noise sources are speckle and instrument noise (Wuttge and Munz, 1995) and, in the present model, azimuthal effects. If we blindly take the difference $\sigma_{fore}^0 - \sigma_{aft}^0$ or $\sigma_{aft}^0 - \sigma_{fore}^0$ from both ascending and descending passes then we simulate the impact of an “unknown” azimuth angle on σ^0 . The standard deviation of the resulting values which are stored in the random variable ϑ is

$$S(\vartheta) = \sqrt{2} \cdot S(\sigma^0) \quad 6$$

because the variance of a linear combination of mutually independent, normally distributed variables is the sum of their variances. The observation that ϑ is normally distributed in the logarithmic range is the justification for assuming that σ_{fore}^0 and σ_{aft}^0 are normally distributed (Fig. 9).

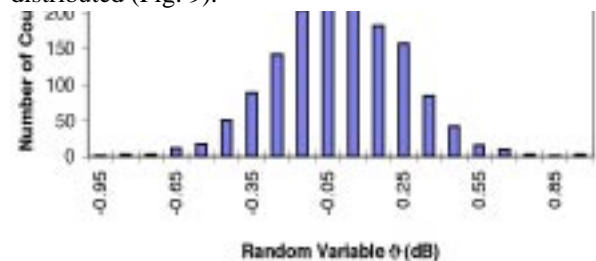


Figure 9: Histogram of the random variable ϑ which has been calculated by first calculating the difference $\delta = \sigma_{fore}^0 - \sigma_{aft}^0$ for both ascending and descending passes and then multiplying δ by +1 or -1 in a random fashion.

Data for this example were taken from a region in Southern Portugal

Since, in reality, the azimuth angle is not random but is determined by the orbit characteristics of the ERS satellites, Equation 6 is not entirely correct. To express this fact we call the derived value for the standard deviation of σ^0 the estimated standard deviation, $\widehat{S}(\sigma^0)$:

$$\widehat{S}(\sigma^0) = \frac{S(\vartheta)}{\sqrt{2}} \quad 7$$

In Equation 10, an overlay of $\widehat{S}(\sigma^0)$ over a DEM of the Iberian Peninsula is shown. About half of the values of $\widehat{S}(\sigma^0)$ - which can mainly be found in more gently sloping terrain - are in the range 0.15 - 0.2 dB and the other half is above 0.2 dB with the highest values found in the Pyrenees.

Influence of Land Cover on Noise Level

Experience has shown that $\widehat{S}(\sigma^0)$ is not only related to large-scale terrain features but also to land cover. For example, $\widehat{S}(\sigma^0)$ is in general smaller over forested areas than over regions with low vegetation cover. This is because azimuthal effects are in principle incidence angle effects and consequently $\widehat{S}(\sigma^0)$ is lower over forested areas where σ^0 decreases more slowly with the incidence angle than over grass- and agricultural land. Also, $\widehat{S}(\sigma^0)$ is observed to be high over areas with large water bodies. To investigate the dependency of $\widehat{S}(\sigma^0)$ on land cover in more detail a multiple correlation analysis between $\widehat{S}(\sigma^0)$ and the area occupied by CORINE land cover classes within one ERS Scatterometer pixel is conducted. The CORINE Programme (Co-ordination of Information on the Environment) has been realised by the European Commission and one of its major tasks is the establishment of a computerised inventory on the land cover. On the most detailed level the CORINE land cover consists of 44 class. For the present analysis a subset of these 44 classes was taken and was grouped into only four class: artificial surfaces including urban areas and other build-up areas, inland waters, open spaces with little or no vegetation, and low vegetation including agricultural- and grassland (Table

2). To make inferences about the dependency of $\widehat{S}(\sigma^0)$ on these four classes a multiple regression together with a one-sided t-test for each regressor is performed. The multiple coefficient of determination is low ($R^2 = 23\%$) but significant. For all classes the null hypothesis that the regressor is equal to zero can be rejected with high confidence, at the $\alpha = 0.5\%$ level for the “inland water” class and at the $\alpha = 0.05\%$ level for the other three classes. Thus it can be concluded:

1. Most of the variation of $\widehat{S}(\sigma^0)$ is caused by terrain effects but also land cover classes are important for the explanation of $\widehat{S}(\sigma^0)$.
2. The magnitude of azimuthal effects depends on how fast σ^0 decreases with the incidence angle because, as shown previously, azimuthal effects are in reality incidence angle effects. Since σ^0 decreases quickly with the incidence angle over sparsely vegetated areas, $\widehat{S}(\sigma^0)$ tends to be higher over areas with sparse or low vegetation cover than over forested regions.
3. The noise level increases with the percent area occupied by build-up areas and water bodies. This is because both surface types show azimuthal behaviour

Classes	CORINE class	% of total area of the Iberian Peninsula
Artificial surfaces (%)	1.	1.3
Inland waters (%)	5.1.	1.3
Open spaces with little or no vegetation	3.3	6.7
Arable land and natural grassland	2.1.1 + 3.2.1	24.6

Table 2: Corine classes used for multiple regression analysis

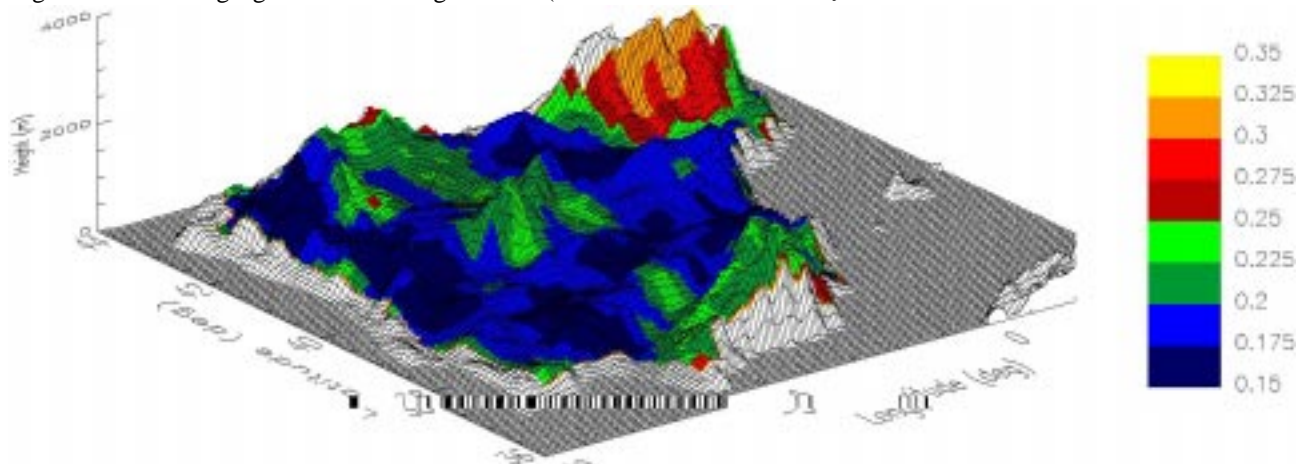


Figure 10: Overlay of the estimated standard deviation of σ^0 , $\widehat{S}(\sigma^0)$, in dB over the DEM of the Iberian Peninsula.

Estimating the Noise Level due to Instrument Noise and Speckle

Because $\widehat{S}(\sigma^0)$ can be as low as 0.15 dB the standard deviation of σ^0 due to instrument noise and speckle effects alone must be even better than that. This value is on the low side of specifications found in the literature. To investigate the noise level of ERS Scatterometer measurements it is generally assumed that backscatter from tropical forests is stable. For example, by analysing σ^0 separately for each antenna and separately for ascending and descending passes Frison and Mougin (1996b) found that σ^0 is stable with an estimated standard deviation smaller than 0.22 dB for all beams and passes. However, even over tropical rain forests, σ^0 shows variations in the magnitude of 0.5 dB to 1 dB due to precipitation (Fig. 7, Wismann et al., 1996) and other environmental effects. Therefore this classical approach overestimates the relative noise level of ERS Scatterometer measurements. On the other side, environmental factors play no role in the calculation of $\widehat{S}(\sigma^0)$ thus allowing a better estimate of the standard deviation of σ^0 due to instrument noise and speckle. Azimuthal effects are not important over tropical forests because σ^0 decreases only slightly with the incidence angle. As can be seen in Fig. 11 which shows over the african rain for-

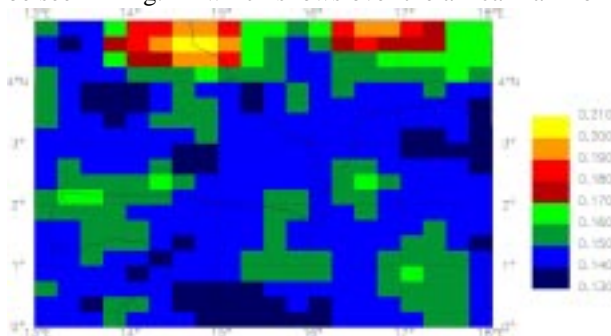


Figure 11: The estimated standard deviation of σ^0 , $\widehat{S}(\sigma^0)$ in dB over the tropical forest in Africa. The area shown covers partly Congo, Cameroon, Central African Republic and Gabon.

est the standard deviation of σ^0 due to instrument noise and speckle is about 0.13 dB. Any increase over this value is due to azimuthal effects.

Given that $\widehat{S}(\sigma^0)$ may be as large as 0.5 dB it becomes clear that azimuthal effects are important and must be considered in any error analysis of ERS Scatterometer land data. $\widehat{S}(\sigma^0)$ itself can be used in various ways, e.g. to define criteria to reject invalid ERS Scatterometer measurements which might occur during instrument switching operations (Wuttge and Munz, 1996) or to provide an error estimate of any geophysical product derived from ERS Scatterometer data.

Conclusions

In this paper it was described how high quality ERS Scatterometer products can be ensured. While an absolute calibration and validation of ERS Scatterometer data is carried out by ESA, product developers may assess the relative noise level of these data by themselves. As shown in this paper azimuthal effects caused by large scale terrain features, inland waters, and build-up areas have an impact on ERS Scatterometer measurements. A simple method was presented that allows to assess the relative noise level of σ^0 due to instrument noise, speckle, and azimuthal effects. The method is unique in that no external data sets are required. The procedures introduced here can also be applied for future scatterometers like the planned Advanced Scatterometer (ASCAT) on METOP.

References

- [1] Amans V. (1996) ERS Wind Scatterometer Quality Control, NOAA/NESDIS Workshop Proceedings, April 1996, Alexandria, VA, USA.
- [2] Attema E. (1989) Estimating Satellite Pointing Biases from Scatterometer transponders Measurements - An exact Solution, ORM/3078/EA/sml, 14 March 1989.
- [3] Attema E. (1996) The Design, Calibration and System Performances of the ERS-1 and ERS-2 Wind Scatterometer, NOAA/NESDIS Workshop Proceedings, April 1996, Alexandria, VA, USA.
- [4] Boehnke K., V. R. Wismann (1996) ERS Scatterometer Land Applications: Detecting Soil Thawing in Siberia, Earth Observation Quarterly, N 52.
- [5] Cavanié A., P. Lecomte (1987) Study of a method to dealise winds from ERS-1 data, ESA contract 6874/87/GP-I(sc), 1987.
- [6] Frison P. L., E. Mougin (1996a) Monitoring global vegetation dynamics with ERS-1 wind Scatterometer data, Int. J. Remote Sensing, Vol. 17, No. 16, pp. 3201-3218.
- [7] Frison P. L., E. Mougin (1996b) Use of ERS-1 Wind Scatterometer data over Land Surfaces, IEEE Trans. Geosc. Remote Sensing, Vol. 34, No. 2, pp. 550-560.
- [8] Graham R. et Al. (1989) Evaluation of ERS-1 Wind Extraction and Ambiguity Removal Algorithms, ESA Contract, January 1989.
- [9] Guyenne D. ed. (1989) ERS-1 A new tool for global environmental monitoring in the 1990's, ESA BR-36, November 1989, ESTEC, Noordwijk. The Netherlands, (ISBN 92-9092-019-X).

- [10]Lecomte P. et Al. (1995) ERS product Assurance and Quality Control, ESA Bulletin 82, May 1995, ESTEC, Noordwijk, The Netherlands, (ISSN) 0376-4265).
- [11]Lecomte P., Attema E.P.W. (1992) Calibration and Validation of the ERS-1 Wind Scatterometer, Proc. First ERS-1 Symposium, 4-6 November 1992, Cannes, France.
- [12]Lecomte P. (1993) CMOD4 Model Description, ESA technical note ER-TN-ESA-GP-1120, Rev. 1.2, March 1993.
- [13]Long A.E. (1985), Toward a C-Band Radar Sea Echo model for the ERS-1 Scatterometer, Proc. of the Third international Colloquium on Spectral Signature of Objects in Remote Sensing, les Arcs 1985, ESA SP-247, ESTEC, Noordwijk. The Netherlands, (ISSN 079-6566).
- [14]Long A.E. (1991) ERS-1 C-Band and Sea-Echo Models, ESA internal Report ESTEC/WMA/9104, Rev. 1. April 1991.
- [15]Longdon N. ed. (1991) ERS-1 Data Book, ESA BR-75, April 1991, ESTEC, Noordwijk. The Netherlands, (ISSN 0250-1589).
- [16]Magagi R.D., Y.H. Kerr (1997a) Retrieval of soil moisture and vegetation characteristics by use of ERS-1 wind Scatterometer over arid and semi arid areas, J. Hydrology, No. 188-189, pp. 361-384.
- [17]Mestre O. (1993) Réponse du diffusiomètre d'ERS-1 en fonction de l'angle d'incidence, note de travail de L'ENM 462.
- [18]Offiler D. (1996) Validation of ERS-1 Scatterometer Winds; An appraisal of Operational Backscatter Model Performances from launch to Present, NOAA/NESDIS Workshop Proceedings, April 1996, Alexandria, VA, USA.
- [19]Pulliainen J., J. Grandell, M. Hallikainen, M. Virtanen, N. Walker, S. Metsaemaeki, J.P. Ikonen, Y. Sucksdorff, T. Manninen (1996b) Scatterometer and Radiometer Land Applications, ESRIN Contract: 11122/94/I-HGE(SC), 253 p.
- [20]Rott H., H. Miller, K. Sturm, W. Rack (1993) Application of ERS-1 SAR and Scatterometer Data for Studies of the Antarctic Ice Sheet, Proc. Second ERS-1 Symposium - Space at the service of our environment, Hambourg 1993, ESTEC, Noordwijk. The Netherlands, (ISBN 92-9092-286-9).
- [21]Stoffelen, A. (1997);Improvement and Quality Assurance of the scatterometer Wind Product in the Backscatter Domain. Proceedings of the CEOS Wind and Wave Validation Workshop, ESA WPP-147, 159-160.
- [22]Stoffelen, A., Gaffard, C. and D. Anderson (1993): ERS-1 Scatterometer data assimilation. Proc. of the Second ERS-1 Symposium - Space at the service of our environment, Hambourg 1993, ESA SP-361, ESTEC, Noordwijk. The Netherlands, (ISBN 92-9092-286-9).
- [23]Stoffelen, A., D. Anderson (1993): Characterisation of ERS-1 Scatterometer measurements and wind retrieval. Proc. of the Second ERS-1 Symposium - Space at the service of our environment, Hambourg 1993, ESTEC, Noordwijk. The Netherlands, (ISBN 92-9092-286-9).
- [24]Vass P., B. Battrick ed.(1992) ERS-1 System, ESA SP-1146, September 1992, ESTEC, Noordwijk. The Netherlands, (ISSN 0379-6566).
- [25]Wagner W. (1996) Change Detection with the ERS Scatterometer over Land, EWP N 1896, ESA ESTEC, Noordwijk, 143 p.
- [26]Wagner W. (1998) Vegetation Cover Effects on ERS Scatterometer Data, Technical Note No. I.98.05, Space Applications Institute, EC Joint Research Centre, Ispra, Italy, 193 p.
- [27]Wagner W., M. Borgeaud, J. Noll (1996) Soil Moisture Mapping with the ERS Scatterometer, Earth Observation Quarterly, N 54, pp. 4-7.
- [28]Wagner W., J. Noll, M. Borgeaud, H. Rott (1998) Monitoring Soil Moisture over Canadian Prairies with the ERS Scatterometer, IEEE. Geosc. Remote Sensing, in press.
- [29]Wismann V. R., K. Boehnke (1994) Land surface monitoring using the ERS-1 Scatterometer, Earth Observation Quarterly, N 44, pp. 11-15.
- [30]Wooding M. ed. (1992) ERS-1 Geophysical Validation, Workshop Proc., ESA WPP-36, August 1992, ESTEC, Noordwijk. The Netherlands.
- [31]Wuttge S., H. Munz (1995) Effects of Gaps in Scatterometer Raw Data on s0- Triplets, ESA, Doc. No. ER-TN-DSF-FL-0001, 95 p.
- [32]Wismann V., K. Boehnke, A. Cavanié, R. Ezraty, F. Gohin, D. Hoekman, I. Woodhouse (1996) Land Surface Observations using the ERS-1 Windscatterometer, Part II, ESA ESTEC, Contract No. 11103/94/NL/CN, 59 p.